Gravitational-wave astronomy with LIGO/Virgo: the SPINSPIRAL code

Marc van der Sluys

University of Alberta, Edmonton / CITA

Vivien Raymond, Ilya Mandel, Vicky Kalogera
Christian Röver, Nelson Christensen, Alberto Vecchio

Outline

Gravitational waves

GWs:

- “Ripples in spacetime”
- Predicted by Einstein’s theory of General Relativity
- *Indirectly* observed for the Hulse-Taylor binary pulsar:

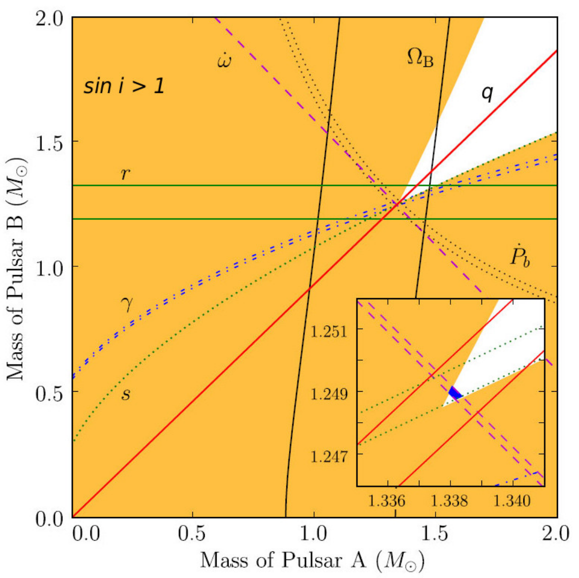

(Breton et al., Science, 2008)

Electromagnetic vs. gravitational waves

EM:

- are waves that propagate through spacetime
- are produced incoherently by many (small) atoms
- have a short wavelength compared to the source size
- use the relatively strong EM force
- have frequencies $\gtrsim 10^6$ Hz
- are measured by energy $\rightarrow \quad L(r) \sim 1/r^2$

GW:

- are waves in the metric of spacetime
- are produced coherently by a few large masses
- have a long wavelength compared to the source size
- use the weak gravitational force
- have frequencies $\lesssim 10^3$ Hz
- are measured by amplitude $\rightarrow \quad L(r) \sim 1/r$

Why detect them?

Physics:

- direct measurement of GWs and verification of GR
- direct observation of black holes
- verify that GWs travel at the speed of light, *i.e.* that the graviton rest mass = 0
- verify that GWs act transversely, *i.e.* that the graviton spin = 2

Astrophysics:

- whole new window to the universe!
- the ripping apart of neutron stars, their implosion to a black hole
- black holes eating neutron stars, BH-BH collisions
- core-collapse supernovae
- hills on pulsars
- primordial GWs as a probe to the Big Bang
- the unexpected

Gravitational waves

Einstein's field equations (1915)

- Matter and energy tell spacetime how to curve ($G = c = 1$):

$$R_{\mu\nu} - \frac{1}{2} R \, g_{\mu\nu} = 8\pi T_{\mu\nu}$$

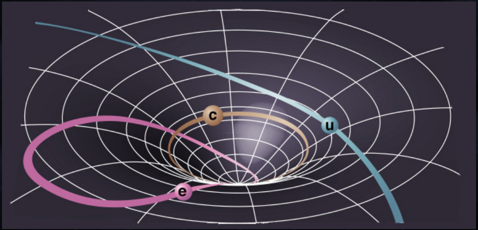

- Curved spacetime tells matter and energy how to move:

$$ds^2 = (\eta_{\mu\nu} + h_{\mu\nu}) \; dx^\mu \, dx^\nu$$

(with $\eta_{\mu\nu}$ the Minkowski metric and $h_{\mu\nu}$ a metric perturbation).

Gravitational waves

- In the weak-field limit, $h \ll 1$ and

$$\left(-\frac{\partial^2}{\partial t^2} + \nabla^2\right) \bar{h}^{\mu\nu} = -16\pi T^{\mu\nu}.$$

- In vacuo, $T^{\mu\nu} = 0$ and the wave equation becomes

$$\left(-\frac{\partial^2}{\partial t^2} + \nabla^2\right) \bar{h}^{\mu\nu} = 0,$$

with the solution

$$\bar{h}^{\mu\nu} = \begin{pmatrix} h_+ & h_\times \\ h_\times & -h_+ \end{pmatrix}.$$

- Note, that:
  - $v = 1 \equiv c$
  - $h_{+,\times}(r) \propto 1/r$

Gravitational waves

Gravitational waves. . .

- propagate transversely at the speed of light
- are quadrupole radiation at the lowest order
- stretch and squeeze spacetime in two polarisations
- allow us to measure their amplitude

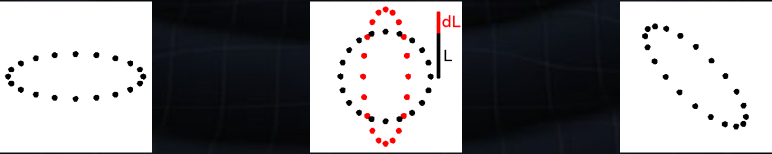

- Strain: $h(t) = h_{+}(t)F_{+}(t) + h_{\times}(t)F_{\times}(t) = \frac{\delta L(t)}{L} \sim 10^{-22}$

Laser Interferometer GW Observatory (LIGO)

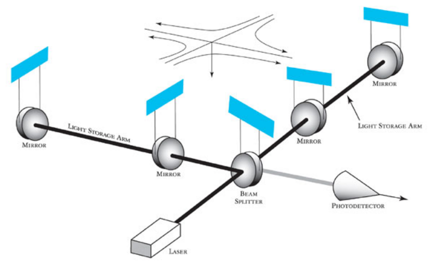

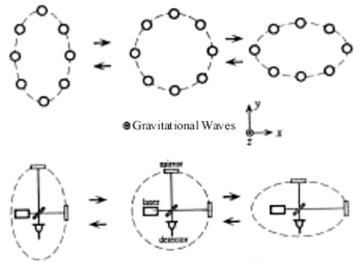

LIGO/Virgo

- LLO: Livingston, Louisiana (L1: 4 km)
- LHO: Hanford, Washington (H1: 4 km, H2: 2 km)
- Virgo: Pisa, Italy (V: 3 km)
- AIGO: western Australia (20??, 5 km)

- Michelson interferometers
- Frequency sensitivity: $f \sim 40 - 1600$ Hz
- $\delta L = 10^{-22} \times L \approx 10^{-16}$ cm (atomic nucleus $\sim 10^{-13}$ cm)

LIGO/Virgo collaboration (LVC):

- Data sharing since spring 2007
- Working groups:
  - Compact binary coalescences
  - Bursts
  - Continuous waves
  - Stochastic background

Inspiral waveforms with increasing spin

LIGO and Virgo detect the last $\sim 10\,$s of a binary inspiral:

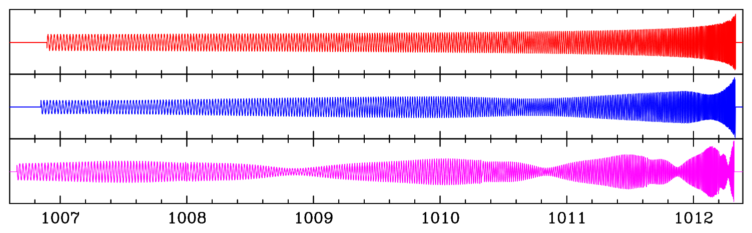

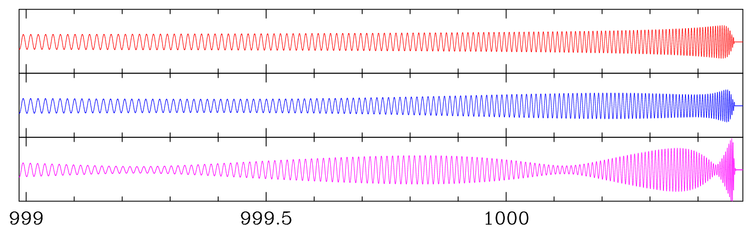

$a_{\mathrm{spin}} \equiv S/M^2 = 0.0, 0.1$ and 0.5

Predicted detection rates

Realistic estimate:

	Rates (yr^{-1})			Horizon (Mpc)		
	NS-NS	BH-NS	BH-BH	NS-NS	BH-NS	BH-BH
Initial	0.015	0.004	0.01	32	67	160
Enhanced	0.15	0.04	0.11	71	149	349
Advanced	20	5.7	16	364	767	1850

Plausible, optimistic estimate:

	Rates (yr^{-1})			Horizon (Mpc)		
	NS-NS	BH-NS	BH-BH	NS-NS	BH-NS	BH-BH
Initial	0.15	0.13	1.7	32	67	160
Enhanced	1.5	1.4	18	71	149	349
Advanced	200	190	2700	364	767	1850

Estimates assume $M_{\rm NS} = 1.4\, M_\odot$ and $M_{\rm BH} = 10\, M_\odot$

CBC group, rates document

Goals for SPINSPIRAL

LIGO

- Show that Markov-Chain Monte Carlo (MCMC) with a large number of parameters (12–15) on LIGO data can be done
- Automated parameter estimation on detected inspiral signal:
  - Confirm spinning inspiral nature of signal
  - Determine *physical* parameters (masses, spin, position, . . .)
- Practise on software and hardware *injections*

Astrophysics

- BH/NS mass distributions, BH spins and spin alignments
- Merger rates, NS-NS/BH-NS/BH-BH merger ratios
- Gravity in strong regime; NS EoS
- Association of GW and EM events, *e.g.* GRB

- Evolution of massive stars (in binaries), CEs
- Initial-mass range for BH progenitors

Signal injection into detector noise

Example:

- Using two 4-km detectors H1, L1
- Gaussian, stationary noise or LIGO/Virgo detector data
- Do software injections
- Retrieve physical parameters
- ΣSNR = 17

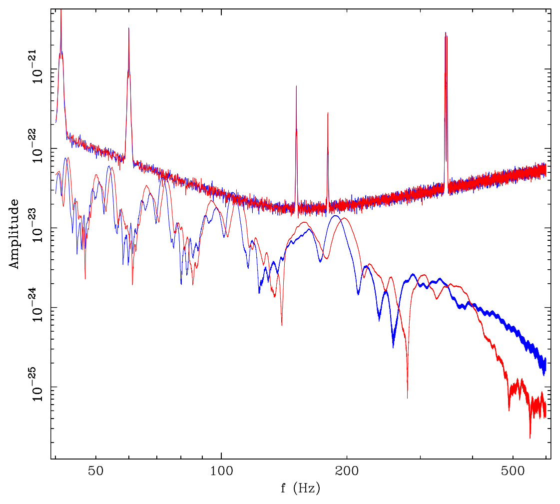

Compute posterior distribution

- Find posterior density of the parameter set $\vec{\lambda}$ that describes the model m
- Bayesian approach, maximum-likelihood method
- The likelihood for each detector i is:

$$L_i(d|\vec{\lambda}) \propto \exp\left(-2\int_0^\infty \frac{\left|\tilde{d}(f) - \tilde{m}(\vec{\lambda},f)\right|^2}{S_n(f)}\,\mathrm{d}f\right)$$

- Coherent network of detectors:
  - $\mathrm{PDF}(\vec{\lambda}) \propto \mathrm{prior}(\vec{\lambda}) \times \prod_i L_i(d|\vec{\lambda})$

- Use Markov-Chain Monte Carlo to sample the posterior

Markov-chain Monte Carlo

- Choose starting point for chain: $\vec{\lambda}_1$
- Compute its likelihood: $L_j \equiv L(d|\vec{\lambda}_j)$ and prior: $p_j \equiv p(\vec{\lambda}_j)$
- do $j = 1, N$
  - draw random jump $\Delta\vec{\lambda}_j$ from Gaussian with width $\vec{\sigma}$
  - consider new state $\vec{\lambda}_{j+1} = \vec{\lambda}_j + \Delta\vec{\lambda}_j$
  - calculate $L_{j+1} \equiv L(d|\vec{\lambda}_{j+1})$ and $p_{j+1} \equiv p(\vec{\lambda}_{j+1})$
  - if($\frac{\mathbf{p_{j+1}}}{\mathbf{p_j}} \frac{\mathbf{L_{j+1}}}{\mathbf{L_j}} >$ **ran_unif[0,1]**) then
    - Accept new state $\vec{\lambda}_{j+1}$
  - else
    - Reject new state; $\vec{\lambda}_{j+1} = \vec{\lambda}_j$
  - end if
  - save state $\vec{\lambda}_{j+1}$
- end do (j)

SPINSPIRAL example

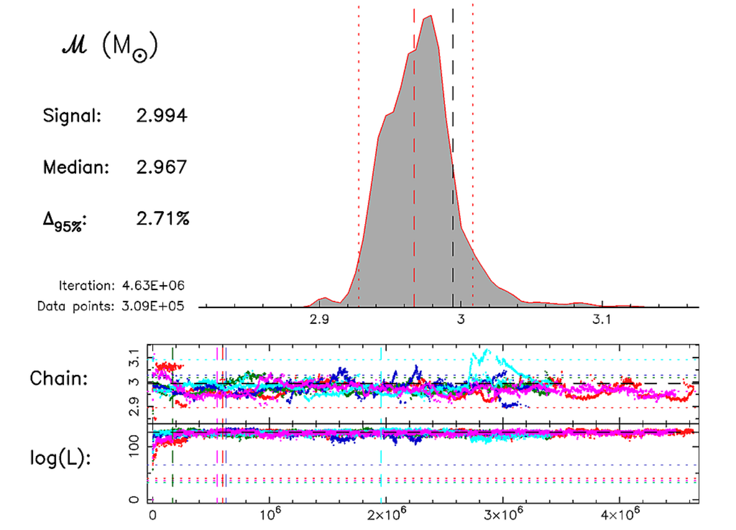

Convergence of chains

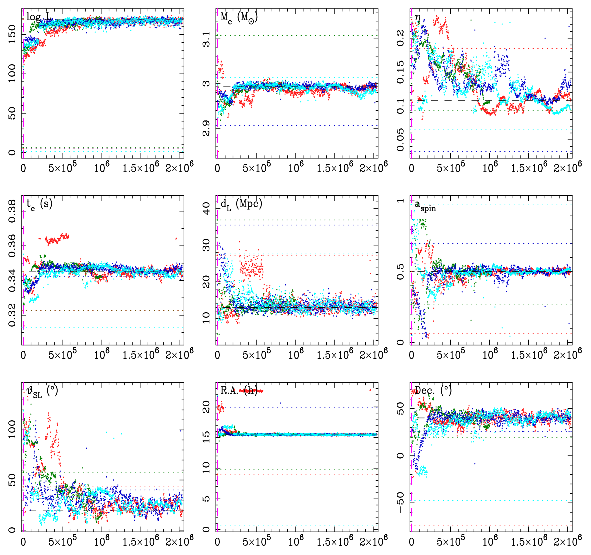

- Dots: starting values
- Dashes: injection values

Correlations increase with spin

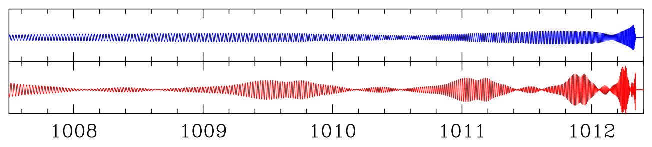

	M_c	η	a_{spin}	ϑ_{SL}	R.A.	Dec.
M_c		0.22	0.42	0.17	−0.40	0.19
η	−0.27		−0.34	−0.53	−0.07	−0.04
a_{spin}	−0.61	0.89		−0.04	0.11	0.62
ϑ_{SL}	0.66	−0.87	−0.99		0.02	−0.34
R.A.	−0.36	0.01	0.02	−0.02		0.12
Dec.	−0.23	0.08	0.18	−0.20	−0.05	

Parameters:

- BH-NS
- H1 & L1
- $M_1 = 10\, M_\odot$
- $M_2 = 1.4\, M_\odot$
- $d_L = 13\,\mathrm{Mpc}$
- $a_{spin} = 0.1, 0.8$
- $\theta_{SL} = 55°$
- Network SNR $\approx 18.2, 30.5$

Parallel tempering

Parallel chains

- Use ~ 5 parallel chains of temperatures $T = 1, \ldots, T_{\text{max}}$
- Acceptance probability for chain with temperature T: $\left(\frac{L_{j+1}}{L_j}\right)^{\frac{1}{T}}$
- Hotter chains explore wider ranges, at lower likelihood
- Probability for swap between chains: $\left(\frac{L_h}{L_c}\right)^{\frac{1}{T_c} - \frac{1}{T_h}}, \quad T_h > T_c$
- Hotter chains pass information to cooler chains

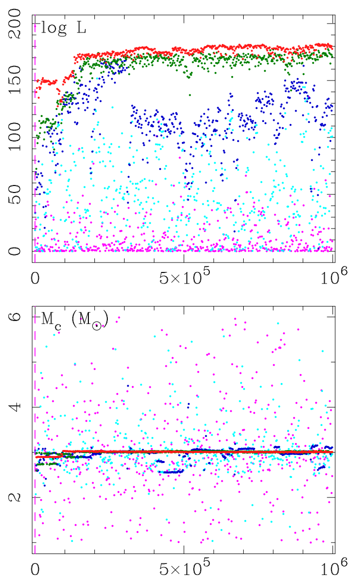

MCMC analyses

MCMC parameters

Masses: $\mathcal{M} \equiv (M_1 + M_2)\,\eta^{3/5}$ & $\eta \equiv \frac{M_1 M_2}{(M_1+M_2)^2}$, distance: $\log d_\mathrm{L}$, time and phase at coalescence: t_c & φ_c, position: α & $\sin\delta$, spin magnitude: $a_{\mathrm{spin}_{1,2}}$, spin orientation: $\cos\theta_{\mathrm{spin}_{1,2}}$ & $\varphi_{\mathrm{spin}_{1,2}}$ & binary orientation: $\cos(\iota)$ & ψ

MCMC set-up

- ≥ 5 serial chains per run, starting from offset parameter values
- Chain length: $\sim$ few $\times 10^6$ states; burn-in: $\sim$ few $\times 10^5$ states
- Run time: 10 days on a 2.8 GHz CPU for 1.5-pN waveform; $\sim 2.5\times$ longer for 3.5-pN

MCMC analyses

MCMC parameters

Masses: $\mathcal{M} \equiv (M_1 + M_2)\,\eta^{3/5}$ & $\eta \equiv \frac{M_1 M_2}{(M_1+M_2)^2}$, distance: $\log d_{\rm L}$, time and phase at coalescence: $t_{\rm c}$ & $\varphi_{\rm c}$, position: α & $\sin\delta$, spin magnitude: $a_{{\rm spin}_{1,2}}$, spin orientation: $\cos\theta_{{\rm spin}_{1,2}}$ & $\varphi_{{\rm spin}_{1,2}}$ & binary orientation: $\cos(\iota)$ & ψ

MCMC set-up

- $\geq$ 5 serial chains per run, starting from offset parameter values
- Chain length: $\sim$ few $\times 10^6$ states; burn-in: $\sim$ few $\times 10^5$ states
- Run time: 10 days on a 2.8 GHz CPU for 1.5-pN waveform; $\sim 2.5\times$ longer for 3.5-pN

Analysis details: BH-NS signal

- Signals injected in simulated noise for H1L1V @ SNR $\approx$17.0
- Fiducial binary: $M_{1,2} = 10 + 1.4\,M_\odot$, $d_{\rm L} = 16$–23 Mpc
- Spin: $a_{\rm spin} = 0.0, 0.1, 0.5, 0.8$, $\theta_{\rm SL} = 20^\circ, 55^\circ$

MCMC results for the analysis of a BH-NS signal

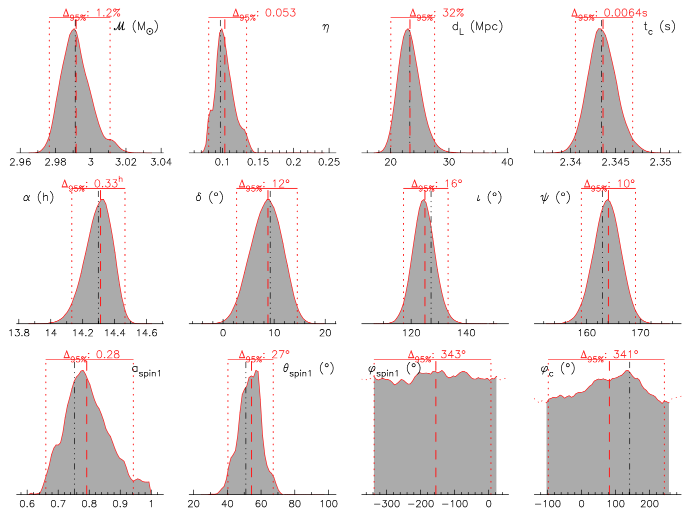

van der Sluys et al., 2008

Parameters:

- H1, L1, V
- $M = 10, 1.4\, M_{\odot}$
- $d_L = 22.4\,\mathrm{Mpc}$
- $a_{\rm spin} = 0.8$, $\theta_{\rm SL} = 55°$
- $\Sigma\mathrm{SNR} \approx 17.0$
- simulated noise

- Black dash-dotted line: injection
- Red dashed line: median
- Δ's: 95% probability

Sky position for signals with different spins

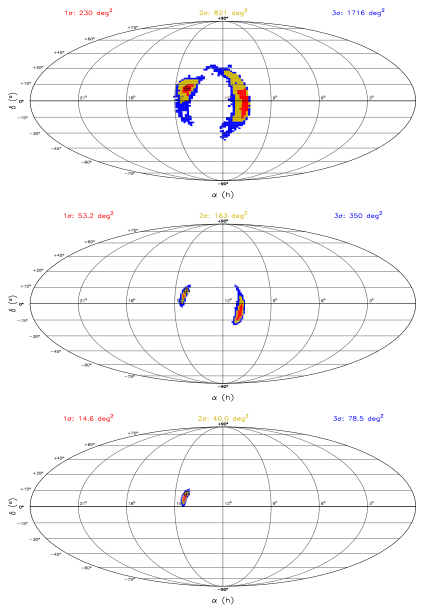

Spinning BH, non-spinning NS:

$10 + 1.4\,M_\odot$, 16–22 Mpc, Σ SNR=17

2 detectors, $a_{\rm spin} = 0.0$

2-σ accuracy: $821^{\circ 2}$

2 detectors, $a_{\rm spin} = 0.5$

2-σ accuracy: $163^{\circ 2}$

3 detectors, $a_{\rm spin} = 0.5$

2-σ accuracy: $40^{\circ 2}$

van der Sluys et al., 2008; Raymond et al., 2009

Accuracy of parameter estimation for BH-NS signals

2 detectors (H1 & V):

a_{spin}	θ_{SL} (°)	d_L (Mpc)	M_1 (%)	M_2 (%)	$\mathcal{M}$ (%)	η (%)	t_c (ms)	d_L (%)	a_{spin}	θ_{SL} (°)	Pos. (°^{2})	Ori. (°^{2})
0.0	0	16.0	95	83	2.6	138	18	86	0.63	—	537	19095
0.1	20	16.4	102	85	1.2	90	10	91	0.91	169	406	16653
0.1	55	16.7	51	38	0.88	59	7.9	58	0.32	115	212	3749
0.5	20	17.4	53[b]	42[a]	0.90	50[b]	5.4	46[a]	0.26	56	111[a]	3467[a]
0.5	55	17.3	31	24	0.62	41	4.9	21	0.12	24	19.8	178[a]
0.8	20	17.9	54[a]	42[a]	0.86[a]	54[a]	6.0	56	0.16	25[a]	104[a]	1540
0.8	55	17.9	21	16	0.66	29	4.7	22	0.15	15	22.8	182[a]

3 detectors (H1, L1 & V):

a_{spin}	θ_{SL} (°)	d_L (Mpc)	M_1 (%)	M_2 (%)	$\mathcal{M}$ (%)	η (%)	t_c (ms)	d_L (%)	a_{spin}	θ_{SL} (°)	Pos. (°^{2})	Ori. (°^{2})
0.0	0	20.5	114	90	2.6	119	15	69	0.98[b]	—	116	4827
0.1	20	21.1	70	57	0.92	72	7.0	60	0.49	160	64.7	3917
0.1	55	21.4	62	48	0.93	68	6.2	51	0.52	123	48.7	976
0.5	20	22.3	54[b]	44[a]	0.89[a]	48[b]	3.3	52	0.28[a]	69	28.8	849
0.5	55	22.0	33	25	0.62	43	4.6	23[a]	0.14	27	20.7	234[a]
0.8	20	23.0	53[b]	41[a]	0.85[a]	52[b]	3.8	55	0.17	23[a]	36.4[a]	645
0.8	55	22.4	30	22	0.86	40	5.0	26	0.21	21	27.2	288

90%-probability ranges, injection SNR = 17.0

[a] the injection value lies outside the 90%-probability range

[b] idem, outside the 99%-probability range, but inside the 100% range

van der Sluys et al., 2008

Analysis of a BH-BH signal without spins

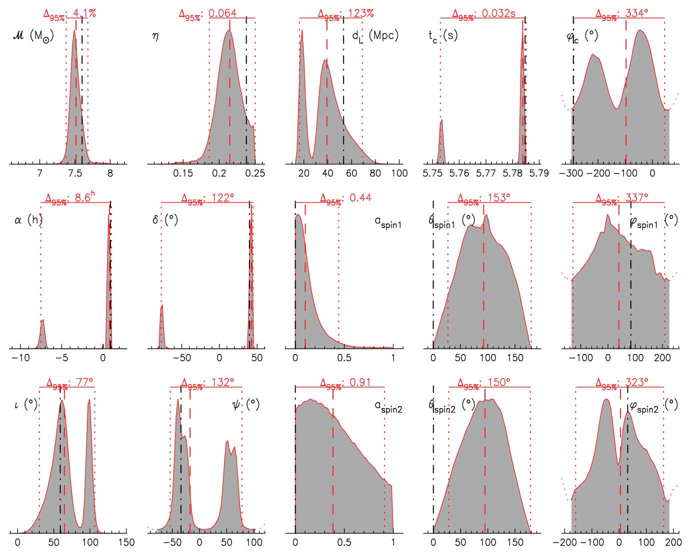

N-2:

- 3.5-pN waveform
- 3 detectors (H1,L1,V)
- $\mathcal{M} = 7.6\, M_\odot$, $\eta = 0.238$; $M_1 = 11.0\, M_\odot$, $M_2 = 7.0\, M_\odot$
- $a_{s1,2} = 0.0$
- $d_L = 53.3$ Mpc
- Σ SNR=15
- simulated noise

van der Sluys et al., in preparation

Analysis of a BH-BH signal with spins

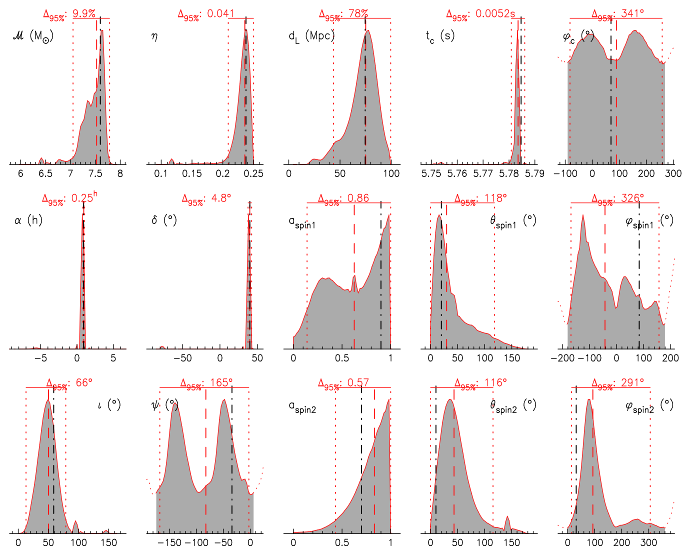

van der Sluys et al., in preparation

HS-2:

- 3.5-pN waveform
- 3 detectors (H1,L1,V)
- $\mathcal{M} = 7.6\,M_\odot$, $\eta = 0.238$; $M_1 = 11.0\,M_\odot$, $M_2 = 7.0\,M_\odot$
- $a_{s1,2} = 0.9, 0.7$
- $\theta_{s1,2} = 10, 20°$
- $d_L = 74.5$ Mpc
- Σ SNR=15
- simulated noise

The importance of having spins in your analysis

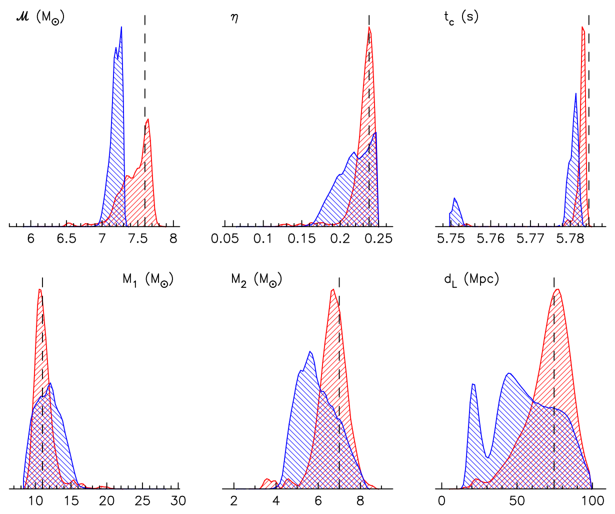

Signal with spins

Analysis with spinning template

Analysis with non-spinning template

van der Sluys et al., in preparation

Accuracy of parameter estimation for BH-BH signals

ID	d_L (Mpc)	$\mathcal{M}$ (%)	η	M_1 (%)	M_2 (%)	d_L (%)	t_c (ms)	a_{s1}	θ_{s1} (°)	a_{s2}	θ_{s2} (°)	Pos. (°^{2})	ψ (°)	ι (°)
N-0	53.3	2.4	0.047	33	34	132	32	–	–	–	–	30.3	142	87
N-1		3.9	0.058	47	43	128	32	0.41	151	–	–	43.3	137	79
N-2		4.1	0.064	50	45	123	32	0.44	153	0.91	150	45.0	132	77
LS-0	59.8	2.0	0.039	34	34	121	32	–	–	–	–	36.8	114	60
LS-1		3.4	0.048	45	41	115	32	0.48	144	–	–	48.1	114	52
LS-2		4.7	0.058	51	43	115	32	0.57	145	0.89	149	53.4	115	51
HS-0	74.5	3.8	0.069	54	54	131	32	–	–	–	–	55.2	158	104
(HS-1		25.1	0.154	92	106	126	34	0.97	139	–	–	81.4	164	93)
HS-2		9.9	0.041	41	40	78	5.2	0.86	118	0.57	116	41.1	165	66
HL-0	62.9	3.2	0.061	50	50	141	32	–	–	–	–	63.9	161	90
(HL-1		10.4	0.111	76	76	67	7.2	0.82	133	–	–	67.6	167	131)
HL-2		6.9	0.037	34	31	28	3.1	0.70	135	0.55	92	37.9	171	166

van der Sluys et al., in preparation

N: non-spinning
LS: low spins, small angles
HS: high spins, small angles
HL: high spins, large angles

low spins: $a_{s1,2} = 0.2, 0.1$
high spins: $a_{s1,2} = 0.9, 0.7$
small angles: $\theta_{s1,2} = 20°, 10°$
large angles: $\theta_{s1,2} = 70°, 50°$

Cetera

LIGO data

- No bias in PE in most cases
- Lower accuracy (when SNR is low)
- Hard to publish

Cetera

LIGO data

- No bias in PE in most cases
- Lower accuracy (when SNR is low)
- Hard to publish

CBC follow-up pipeline

- SPINSPIRAL in the pipeline
- Semi-automatic follow-up possible
- Systematic follow-up of the loudest candidates, hardware injections, etc.

Cetera

LIGO data

- No bias in PE in most cases
- Lower accuracy (when SNR is low)
- Hard to publish

CBC follow-up pipeline

- SPINSPIRAL in the pipeline
- Semi-automatic follow-up possible
- Systematic follow-up of the loudest candidates, hardware injections, etc.

NINJA 1

- Gaussian noise
- High-mass waveforms
- Spin "helps" chirp mass

Cetera

NINJA 2

- LIGO noise
- Lower-mass waveforms
- Add merger and ringdown

Cetera

NINJA 2

- LIGO noise
- Lower-mass waveforms
- Add merger and ringdown

Sky localisation

- MCMC is slow
- MCMC gives “final” answer
- Compare to rapid codes, *e.g.* using triangulation

Cetera

NINJA 2

- LIGO noise
- Lower-mass waveforms
- Add merger and ringdown

Sky localisation

- MCMC is slow
- MCMC gives “final” answer
- Compare to rapid codes, *e.g.* using triangulation

LIGO South

- What is the best location for a fourth detector?
- To what extent does it improve parameter estimation?

Conclusions

GW parameter-estimation code:

We have developed the code SPINSPIRAL which can recover the 12–15 parameters of a binary inspiral, including one or two spins, using a Markov-chain Monte-Carlo technique

Conclusions

GW parameter-estimation code:

We have developed the code SPINSPIRAL which can recover the 12–15 parameters of a binary inspiral, including one or two spins, using a Markov-chain Monte-Carlo technique

Accuracies for the analysis of a BH-NS signal with $q \approx 0.14$ and SNR ≈ 17:

- The presence of spin in the BH increases the accuracy of parameter estimation
- In this case, we can produce astronomically relevant information, with typical accuracies for lower / higher spin:
  - individual masses: $\sim$ 30–40%
  - dimensionless spin: $\sim$ 0.6 / 0.2
  - distance: $\sim$ 40–60%
  - sky position: $\sim 100^{\circ^2}$ / 30°^2} (3 detectors)
  - binary orientation: $\sim 2500^{\circ^2}$ / 400°^2} (3 detectors)
  - time of coalescence: $\sim$ 10 ms / 5 ms

Conclusions

Accuracies for analysis of a BH-BH signal with $q \approx 0.63$ and SNR ≈ 15:

- The typical accuracies using data from 3 detectors, for lower / higher spin:
  - individual masses: $\sim 50\%$
  - individual spins: ~ 0.6
  - distance: $\sim$ 120% / 50%
  - sky position: $\sim 45^{\circ 2}$
  - time of coalescence: $\sim$ 30 ms / 4 ms
- These accuracies can lead to association with an electromagnetic detection (*e.g.* gamma-ray burst)

Conclusions

Accuracies for analysis of a BH-BH signal with $q \approx 0.63$ and SNR ≈ 15:

- The typical accuracies using data from 3 detectors, for lower / higher spin:
  - individual masses: $\sim 50\%$
  - individual spins: ~ 0.6
  - distance: $\sim$ 120% / 50%
  - sky position: $\sim 45^{\circ 2}$
  - time of coalescence: $\sim$ 30 ms / 4 ms
- These accuracies can lead to association with an electromagnetic detection (*e.g.* gamma-ray burst)

Inclusion of spin in parameter estimation:

- The inclusion of spin adds a significant number of dimensions and introduces (strong) correlations
- Failing to take into account spin can result to biases in especially mass parameters

End...